


# Climate change impacts on selected global rangeland ecosystem services

Randall B. Boone<sup>1,2</sup>  | Richard T. Conant<sup>1,2</sup> | Jason Sircely<sup>3</sup> | Philip K. Thornton<sup>3</sup> | Mario Herrero<sup>4</sup>

<sup>1</sup>Natural Resource Ecology Laboratory, Colorado State University, Fort Collins, CO, USA

<sup>2</sup>Department of Ecosystem Science and Sustainability, Colorado State University, Fort Collins, CO, USA

<sup>3</sup>CGIAR Research Program on Climate Change, Agriculture and Food Security (CCAFS), International Livestock Research Institute, Nairobi, Kenya

<sup>4</sup>The Commonwealth Scientific and Industrial Research Organization, St. Lucia, QLD, Australia

## Correspondence

Randall B. Boone, Natural Resource Ecology Laboratory, Colorado State University, Fort Collins, CO, USA.

Email: randall.boone@colostate.edu

## Abstract

Rangelands are Earth's dominant land cover and are important providers of ecosystem services. Reliance on rangelands is projected to grow, thus understanding the sensitivity of rangelands to future climates is essential. We used a new ecosystem model of moderate complexity that allows, for the first time, to quantify global changes expected in rangelands under future climates. The mean global annual net primary production (NPP) may decline by  $10 \text{ g C m}^{-2} \text{ year}^{-1}$  in 2050 under Representative Concentration Pathway (RCP) 8.5, but herbaceous NPP is projected to increase slightly (i.e., average of  $3 \text{ g C m}^{-2} \text{ year}^{-1}$ ). Responses vary substantially from place-to-place, with large increases in annual productivity projected in northern regions (e.g., a 21% increase in productivity in the US and Canada) and large declines in western Africa (–46% in sub-Saharan western Africa) and Australia (–17%). Soil organic carbon is projected to increase in Australia (9%), the Middle East (14%), and central Asia (16%) and decline in many African savannas (e.g., –18% in sub-Saharan western Africa). Livestock are projected to decline 7.5 to 9.6%, an economic loss of from \$9.7 to \$12.6 billion. Our results suggest that forage production in Africa is sensitive to changes in climate, which will have substantial impacts on the livelihoods of the more than 180 million people who raise livestock on those rangelands. Our approach and the simulation tool presented here offer considerable potential for forecasting future conditions, highlight regions of concern, and support analyses where costs and benefits of adaptations and policies may be quantified. Otherwise, the technical options and policy and enabling environment that are needed to facilitate widespread adaptation may be very difficult to elucidate.

## KEYWORDS

annual net primary production, forage biomass, global rangeland simulator, G-Range, livestock, plant cover change, plant functional groups

## 1 | INTRODUCTION

Rangelands are Earth's dominant ice-free land cover (Reid, Galvin, & Kruska, 2008) and are important providers of ecosystem services,

such as maintenance of biodiversity (Hobbs et al., 2008), carbon sequestration (Henderson et al., 2015), and satisfying the growing demand for livestock products (Erb et al., 2016; Thornton, 2010). Rangelands are typified by sparse and variable precipitation (Hobbs et al., 2008), diverse vegetation physiology and lifeform, and strong plant–animal interactions.

Rangelands (i.e., areas of vegetation suitable for grazing by herbivores) support the largest land-use system on the planet, feeding

livestock. Rangelands contribute 25%–40% of global small ruminant meat production, 30% of global small ruminant milk production, and 22% and 55% of beef production in Latin America and Oceania, respectively (Herrero, Havlík et al., 2013). In some regions, they also provide significant proportions of cattle milk production (25% in sub-Saharan Africa, for example, Herrero, Havlík et al., 2013). In many developing countries, demand for livestock products from rangelands is projected to increase substantially to the middle of this century, largely as a result of growing populations, increasing urbanization, and rising incomes (Rosegrant et al., 2009). Rangelands also maintain significant bundles of regulating and supporting ecosystems services, particularly carbon storage, water supply, and provide support for biodiversity (Herrero, Wirsensius et al., 2013).

Rangelands maintain the livelihoods of large numbers of people who are vulnerable (e.g., food insecure and poor). About 550 million of the world's poor people (living on less than \$1.25 per day) depend on livestock as one of their few or only assets, and about 58 million of these poor people are in rangelands (Robinson et al., 2011). Levels of poverty and vulnerability in many of the rangelands in developing countries are high (de Leeuw et al., in press). Climate change will increase weather volatility and the frequency of extreme events such as droughts and floods, and the impacts on already vulnerable people are likely to be considerable (Thornton & Herrero, 2014). The links between vulnerability, food security, and climate change are complex, but increased understanding of the likely impacts of climate change on the rangelands is needed to enhance adaptive capacities. Reliance on rangelands is projected to grow, thus understanding the sensitivity of rangelands to future climates is essential (Thornton, 2010). We used a new ecosystem model that allows, for the first time, to quantify in single simulations global changes expected in rangelands under future climates. We used an ensemble of projections from several circulation models to simulate effects of climate change on global rangelands through 2050.

## 2 | MATERIALS AND METHODS

We used a simulation approach to project climate change impacts on rangelands through 2050 at half-degree spatial resolution. We required a global model of intermediate complexity that focused on rangeland plant functional groups rather than crops, allowed functional groups to change in their relative abundance, included grazing and browsing by herbivores, and tracked biogeochemical processes. We developed the global rangeland model G-Range used in these analyses (Boone, Conant, & Hilinski, 2011; Boone, Conant, & Sircey, 2013; Boone, Galvin et al., 2011) after exploring a variety of models to different degrees [e.g., with prime or example citations, SimSAGS (Derry, 2005), MAPSS (Birdsey et al., 1997), IBIS (Foley et al., 1996), the Hurley Pasture Model (Thornley, 1997), Biome-BG (Thornton et al., 2002), GENDEC (Moorhead & Reynolds, 1991), Grazing Lands Application (Stuth et al., 1990), GrazPlan (Moorhead & Reynolds, 1991), PHYGROW (Stuth et al., 2003), SAVANNA

(Coughenour, 1992), and CENTURY (Parton et al., 1993)]. Our review indicated the need for a simulation tool designed to represent plant functional groups in rangelands at moderate resolution (e.g., the globe comprised of grid cells from 1 to 1/12th degree resolution). Existing tools were local rather than global, too simple, too complex, or no longer supported. We created a novel tool that can help set priorities for national, regional, and global decision-making concerning future adaptation and mitigation options in rangelands. We selected CENTURY (Parton et al., 1993) as the foundation for biogeochemical modeling in G-Range, given its common use around the world and history of development at the G-Range author's institution. Aspects of G-Range were influenced by our experience with SAVANNA (Coughenour, 1992; e.g., Boone et al., 2002, 2005; Boone, Galvin et al., 2011; Boone, Conant et al., 2011; Boone & Lesorogol, 2016). Individual-based plant population modeling and some other aspect of G-Range are new contributions. G-Range is programmed in Fortran 95.

The model is supplied with spatial surfaces that describe soil properties and cover for herbaceous plants, shrubs, and deciduous and evergreen trees. Spatial surfaces define cells (0.5 degree  $\times$  0.5 degree simulations are reported here) to be considered rangeland and modeled, and landscape units for which parameters are provided that describe nutrient cycling, plant growth, establishment and plant death, grazing, fire, and fertilization (Boone, Galvin et al., 2011; Boone, Conant et al., 2011; Boone et al., 2013). In this application, layers used include soil properties from the Harmonized World Soil Database (FAO (FAO, IIASA, ISRIC, ISS-CAS, JRC), 2012; i.e., proportion sand, silt, clay, gravel, bulk density, and organic carbon), and proportion cover for herbaceous plants (Hansen et al., 2006), shrubs, and deciduous and evergreen trees (DeFries, Hansen, Townshend, Janetos, & Loveland, 2000; Loveland et al., 2000). We derived the shrub layer from the woody vegetation continuous field information (Hansen et al., 2006) using a fractional multiplier of the woody cover from that source. Parameters describing ecosystem dynamics were provided to G-Range for 15 biomes (Figure S1). The biomes (from Ramankutty & Foley, 1999) included as follows: (i) tropical evergreen forest or woodland, (ii) tropical deciduous forest or woodland, (iii) temperate broadleaf evergreen forest or woodland, (iv) temperate needleleaf evergreen forest or woodland, (v) temperate deciduous forest or woodland, (vi) evergreen or deciduous mixed forest or woodland, (vii) savanna, (viii) grassland or steppe, (ix) dense shrubland, (x) open shrubland, (xi) tundra, (xii) desert, and (xiii) polar, plus two that were later found to contain insufficient rangelands for analyses, boreal evergreen forest or woodland, and boreal deciduous forest or woodland. A second surface with detailed land cover (Loveland et al., 2000) was used to indicate cells within those biomes that were rangeland for which dynamics should be simulated, or non-rangeland cells that were not simulated. A mask describing land versus water was derived from a continental shapefile. Per-cell fire frequencies were calculated from satellite-derived products (Giglio et al., 2010) and provided to G-Range as spatial surfaces. A surface storing latitudes of cell centers is used by G-Range to determine incoming radiation and the timing of seasons. Lastly, a zonal

layer is used by G-Range to assign a unique numeric identifier to each cell in the global surface. Those identifiers are used when saving to, and loading from, files that store the state of spin-up simulations. For model development and spin-up, we used as the main dynamic input monthly precipitation, minimum, and maximum temperature surfaces from 1901 to 2006 from the Climatic Research Unit (CRU) of the University of East Anglia (Mitchell & Jones, 2005). Two-thousand year spin-up simulations used CRU monthly precipitation and minimum and maximum temperature surfaces from 1901 to 2006, repeated as needed.

In G-Range, water and nutrient dynamics are tracked through four soil layers and up to five plant parts, and soil carbon pool tracking follows CENTURY, with fast, intermediate, and passive carbon pools used, plus surface litter carbon tracked (Parton et al., 1993). Plants compete for water, nutrients, light, and space to yield biogeochemical- and population-level changes in annual and perennial herbaceous plants, shrubs, and evergreen and deciduous trees. More than 100 surfaces are produced by G-Range each monthly time-step. An overview and detailed description of the G-Range model is in Appendix S1.

Parameters were set based on values provided with CENTURY, from the literature, or inferred. Inferred parameters were most often those pertaining to whole plant death and regeneration, based on the general vegetation types in biomes. Parameters were then adjusted in an iterative process, with directions and degrees of adjustment informed by results from a sensitivity analysis (Boone et al., 2013). Changes were made to one or a small set of parameters in the direction taken to improve fit and then a simulation ran and a comparison made to a suite of spatial surfaces. Adjustments that improved fit for a given landscape unit were retained, otherwise they were rolled-back. Parameters were adjusted until repeated changes to parameters degraded model fit. In these analyses, fit was assessed using Python scripts to compare G-Range output from the mid-2000s to 11 “observed” spatial surfaces, with the goal of minimizing differences. These surfaces included soil surface temperature (Henderson et al., 2015), snow–water equivalency (Armstrong, Brodzik, Knowles, & Savoie, 2005), annual evapotranspiration (Zhang, Kimball, Nemani, & Running, 2010) and potential evapotranspiration (Henderson et al., 2015), soil total organic carbon (Henderson et al., 2015), plant available soil moisture (Henderson et al., 2015), carbon:nitrogen ratio (Batjes, 2002), live carbon density (Ruesch & Gibbs, 2008), leaf area index (Sietse, 2010), annual net primary productivity (Henderson et al., 2015), and decomposition coefficients (Henderson et al., 2015), which are corrections applied to baseline decomposition that reduce rates associated with conditions such as temperature and water availability. The fitness  $r^2$  values for the baseline model are shown in Figure S2, with eight yielding  $r^2 \geq .85$ , leaf area index  $r^2 = .58$ , carbon:nitrogen at 0.21, and plant available soil moisture at 0.17.

Modeled estimates for aboveground and belowground live biomass, net primary productivity, and other responses were compared to local field observations through space and time, summarized in Appendix S1, and parameters further adjusted. Global- and site-scale

model evaluation in rangelands worldwide found that G-Range produced reasonable rates of biomass production with tolerable errors in comparison with MODIS NPP, which are themselves modeled output (Zhao, Running, Heinsch, & Nemani, 2011), and field NPP estimates, and the distributions of vegetation facets simulated by G-Range generally compared favorably with MODIS-derived (Hansen et al., 2006) global vegetation cover.

In analyses, we used a standalone version of MarkSim to down-scaled results from seven atmospheric-ocean global circulation models (GCMs) considered in the IPCC Fifth Assessment Report (IPCC, 2014), using RCPs 4.5 and 8.5. We used data from the downscaled surfaces, at 0.167 degree (10 min) resolution, from 1971 to 2005, and projected data from 2006 to 2070 for monthly precipitation and minimum and maximum temperature. Surfaces were nearest-neighbor resampled to 0.5 degree. The GCMs used were from the following institutions: (i) Beijing Climate Center, China Meteorological Society (BCC-CSM 1.1; Wu, 2012); (ii) Commonwealth Scientific and Industrial Research Organization and the Queensland Climate Change Centre of Excellence (CSIRO-Mk3.6.0; Collier et al., 2011); (iii) Geophysical Fluid Dynamics Laboratory (GFDL-CM3; Donner et al., 2011); (iv) NASA Goddard Institute for Space Studies (GISS-E2-R; Schmidt et al., 2006); (v) Meteorological Office Hadley Centre (HadGEM2.ES; Collins et al., 2011); (vi) Institut Pierre-Simon Laplace (IPSL-CM5A-LR; Dufresne et al., 2013); and (vii) Atmosphere and Ocean Research Institute, National Institute for Environmental Studies, and Japan Agency for Marine-Earth Science and Technology (MIR-CGCM3; Yukimoto et al., 2012).

A baseline was simulated from 1951 to 2006, used in model fitting, and summarized here. For climate futures, analyses were conducted with plant productivity unchanged in response to  $\text{CO}_2$  concentration, and with plant productivity increased in response to  $\text{CO}_2$  fertilization. Comparison of results where  $\text{CO}_2$  fertilization was enabled or not allowed effects of fertilization quantified in isolation. For simulations of future climate, G-Range can modify plant productivity in response to  $\text{CO}_2$  concentration, which was carried out using Parton, Ojima, Del Grosso, and Keough (2001) and used elsewhere (King, Bachelet, & Symstad, 2013; Pan et al., 1998). Their production correction was

$$1 + (\text{CO}_2\text{ipr} - 1) / (\log_{10}(2) * \log_{10}(\text{CO}_2 \text{ concentration} / 350))$$

where  $\text{CO}_2\text{ipr}$  is the multiplier on plant production of doubling the atmospheric  $\text{CO}_2$  concentration from 350 ppm to 700 ppm and was 1.25. We used future  $\text{CO}_2$  concentrations from RCP 4.5 and RCP 8.5 projections used by IPCC (Meinshausen et al., 2011). We used a more recent baseline date from which to capture  $\text{CO}_2$  fertilization effects (2006) and additional corrections to production versus CENTURY (e.g., a correction for proportion live material per vegetation layer), and so a constant (0.2) was subtracted from the values, such that the RCP 4.5 values spanned from 0.8 historically to 0.915 in 2070, and the RCP 8.5 values spanned from 0.8 to 1.008; we used the same curve for all biomes in this application.

With the aim of reducing dimensionality (i.e., 7 GCMs  $\times$  2 RCPs  $\times$  2 plant responses to increased  $\text{CO}_2$ ), in preliminary analyses,

we visualized the differences in model results for scenarios for a given GCM data set. We mapped on paper each of the average annual responses from 2050 from the simulations using the Beijing Climate Center GCM results. The spatial distribution of changes in response to climate changes was very similar—the amount of change varied under RCP 4.5 and RCP 8.5, and with plants with constant or increasing production in response to increasing CO<sub>2</sub>, but not the spatial patterning. We therefore portray ensemble spatial responses in RCP 8.5 with increasing productivity under increased CO<sub>2</sub>, and other responses (i.e., RCP 4.5, CO<sub>2</sub> not influencing vegetation productivity) have similar spatial patterns.

Twenty-eight simulations spanning from 1951 to 2070 were conducted and stored that represented climate change using combinations of the seven global circulation model projections, two RCPs, and two plant responses (i.e., no increase in plant productivity related to increasing CO<sub>2</sub>, and using the coefficients described above). Surfaces used in analyses were exported to GRIDASCII format using a custom utility and analyzed using scripts in ArcPy and mapped using ArcGIS 10.1 (Redlands, CA, USA).

Spatial results are ensemble averages from the 7 GCMs, showing a given simulated metric for 2000 and the predicted change in 2050. Mean ensemble responses for rangeland cells and spatial standard deviations are given for each selected responses, and percent change for regions of the world was charted. Given global changes in herbaceous production (Table 1) and information of feed quality within biomes<sup>10</sup>, we calculated numbers of megajoules in forage gained or lost. Based on the maintenance requirements of one livestock unit (i.e., LUs; 250 kg body mass; Herrero, Havlík et al., 2013), we

calculated the minimum and maximum change in numbers of animals supported given the change in forage production. Percent change in livestock was calculated from these results and the Gridded Livestock of the World (Robinson et al., 2014). A mean percentage dressed weight (i.e., 52%) was used to calculate the change in kg of meat produced from the differences in LUs supported, then that value was multiplied by a global meat carcass price (\$2.60/kg) to estimate economic changes.

### 3 | RESULTS

Baseline values and mean changes in ensemble results using seven global circulation models are presented for 13 global rangeland ecosystem responses under RCPs 4.5 and 8.5, with and without positive effects of elevated atmospheric CO<sub>2</sub> on plant production (Table 1; fit is summarized in Figure S2, values for the biomes are in Table S2). Combinations of these results quantified the magnitude of changes that may be expected under a changing climate, with and without CO<sub>2</sub> fertilization, for constrained and more liberal emission standards.

We show that mean global annual net primary production (NPP) may decline by 10 g C m<sup>-2</sup> year<sup>-1</sup> (222 g C m<sup>-2</sup> year<sup>-1</sup> spatial SD) in 2050 under Representative Concentration Pathway (RCP) 8.5 (Moss et al., 2008), but herbaceous NPP is projected to increase slightly (3 g C m<sup>-2</sup> year<sup>-1</sup>  $\bar{x}$ , 116 g C m<sup>-2</sup> year<sup>-1</sup> SD). NPP is projected to increase by  $\geq 250$  g C m<sup>-2</sup> year<sup>-1</sup> biomass in much of equatorial South America and central Africa and by  $\geq 100$  g

**TABLE 1** Changes projected in selected ecosystem responses for global rangeland areas under projected climate futures for the year 2050

Response <sup>a</sup>	Units	Baseline	Change, RCP 4.5 <sup>b</sup>		Change, RCP 8.5	
			Fixed	Enhanced	Fixed	Enhanced
ANPP	g m <sup>-2</sup> yr <sup>-1</sup>	234.9 (403.9)	-26.78 (210.55)	-12.79 (214.24)	-29.33 (216.60)	-10.07 (221.52)
HNPP	g m <sup>-2</sup> yr <sup>-1</sup>	92.6 (182.8)	-4.90 (110.52)	0.85 (113.08)	-4.55 (112.08)	3.32 (115.89)
Bare cover	prop.	0.41 (0.39)	0.019 (0.141)	0.023 (0.143)	0.018 (0.141)	0.024 (0.803)
Herb cover	prop.	0.24 (0.29)	-0.017 (0.115)	-0.017 (0.116)	-0.018 (0.115)	-0.019 (0.117)
Shrub cover	prop.	0.23 (0.13)	0.001 (0.045)	-0.002 (0.046)	0.002 (0.046)	-0.001 (0.047)
Tree cover	prop.	0.11 (0.13)	-0.002 (0.034)	-0.004 (0.035)	-0.002 (0.034)	-0.004 (0.036)
Herb LAI	index	1.89 (2.67)	0.090 (1.709)	0.272 (1.792)	0.100 (1.754)	0.357 (1.883)
Shrub LAI	index	0.17 (0.33)	0.028 (0.128)	0.041 (0.141)	0.029 (0.135)	0.048 (0.154)
Tree LAI	index	0.37 (0.68)	0.069 (0.297)	0.098 (0.319)	0.073 (0.314)	0.114 (0.345)
C:N ratio	ratio	12.08 (1.33)	0.118 (0.781)	0.189 (0.784)	0.103 (0.798)	0.197 (0.803)
Soil carbon	g m <sup>-2</sup> yr <sup>-1</sup>	3807 (3046)	-31.9 (809.6)	38.3 (816.3)	-46.5 (814.4)	44.4 (823.1)
Above biomass	g m <sup>-2</sup> yr <sup>-1</sup>	861 (1067)	55.8 (618.8)	135.8 (650.0)	59.0 (645.7)	173.6 (695.7)
Below biomass	g m <sup>-2</sup> yr <sup>-1</sup>	3956 (6437)	-21.8 (2060.9)	205.9 (2147.3)	-75.6 (2134.9)	231.3 (2242.3)

The table summarizes ensemble results from simulations that include plant responses to increasing CO<sub>2</sub> that were either "Fixed" or "Enhanced," which represent responses without and with positive effects of elevated CO<sub>2</sub> on production. Values are means with spatial standard deviations in parentheses.

<sup>a</sup>Responses include annual net primary productivity (ANPP), annual herbaceous net primary productivity (HNPP), the mean proportion of bare, herbaceous, shrub, and tree cover and leaf area index (LAI), carbon to nitrogen ratio, soil total organic carbon (Soil carbon), aboveground total live biomass (Above biomass), and belowground total live biomass (Below biomass).

<sup>b</sup>Changes below the precision of the values reported were rounded to the nearest value (e.g., -0.0003 is shown as -0.001).



$\text{C m}^{-2} \text{ year}^{-1}$  in nearby areas plus along the slopes of the Andes, western Australia, and some temperate northern rangelands (Figure 1). Decreases in  $\text{NPP} \geq 250 \text{ g C m}^{-2} \text{ year}^{-1}$  are forecast to occur in mesic and semi-arid (Guinean and Sudanian) savannas south of the Sahara, southern Africa, eastern Australia, parts of Argentina, and the eastern Great Plains. Areas with  $\text{NPP}$  declines  $\geq 100 \text{ g C m}^{-2} \text{ year}^{-1}$  generally neighbored those areas (Figure 1).

Forage production (represented here by  $\text{HNPP}$ ; Figure 2),  $\text{NPP}$ , and vegetative cover responses to climate change are forecasted to vary substantially from place-to-place (Figures S3–S6 includes changes in 10 ecosystem responses). The declines in  $\text{NPP}$ ,  $\text{HNPP}$ , and biomass across much of Africa are evident, as are declining  $\text{NPP}$  in Australia and loss of vegetation cover. Vegetation productivity in northern landscapes is projected to increase, as others have

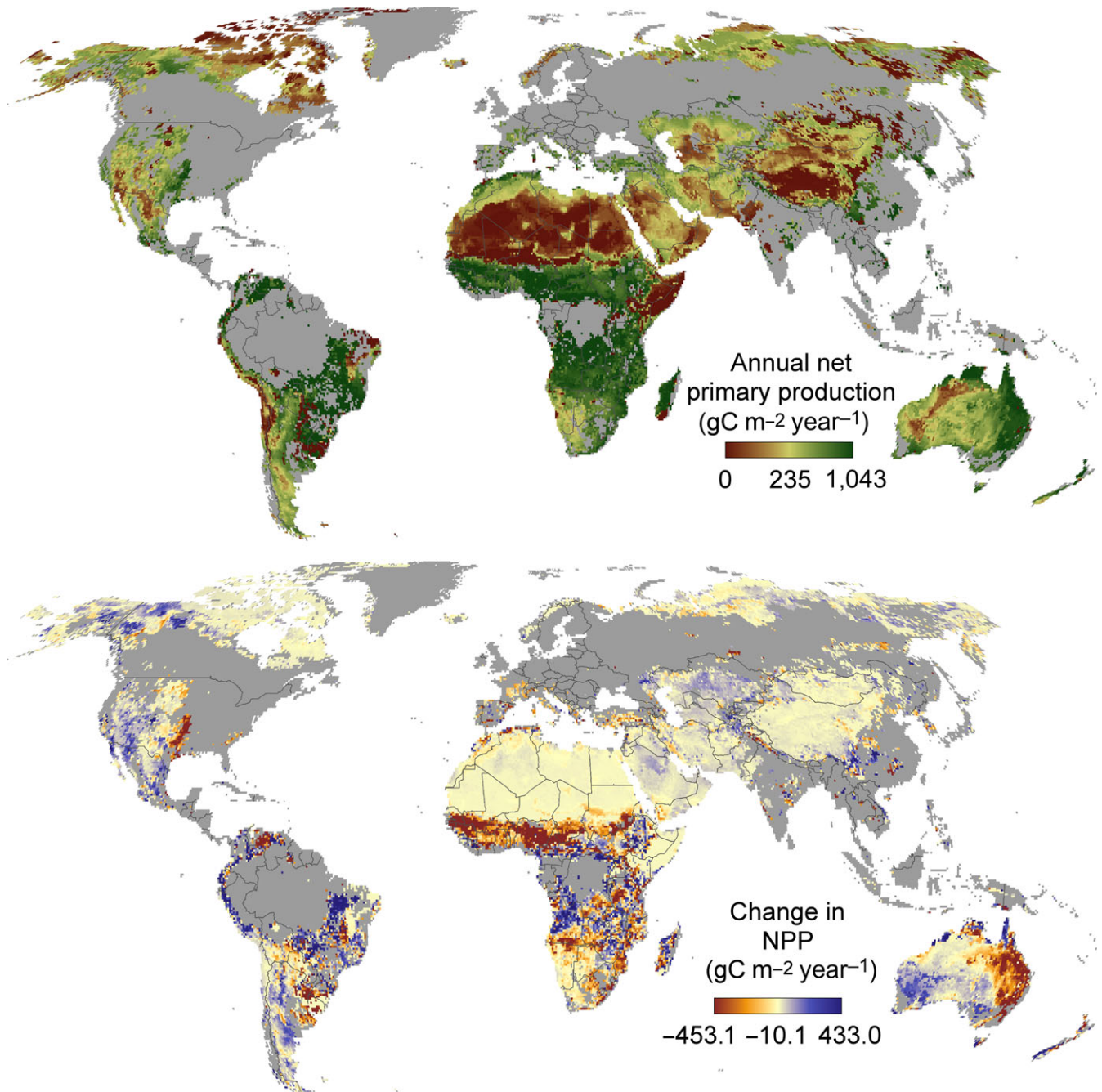


**FIGURE 1** Ensemble simulation results for annual net primary productivity of rangelands as simulated in 2000 (top) and their change in 2050 (bottom) under emissions scenario RCP 8.5, with plant responses enhanced by  $\text{CO}_2$  fertilization. Results from RCP 4.5 and 8.5, with and without positive effects of atmospheric  $\text{CO}_2$  on plant production, differed considerably in magnitude but had similar spatial patterning, and so results from RCP 8.5 with increasing production are portrayed spatially here and in other figures. Scale bar labels and the stretch applied to colors are based on the spatial mean value plus or minus two standard deviations

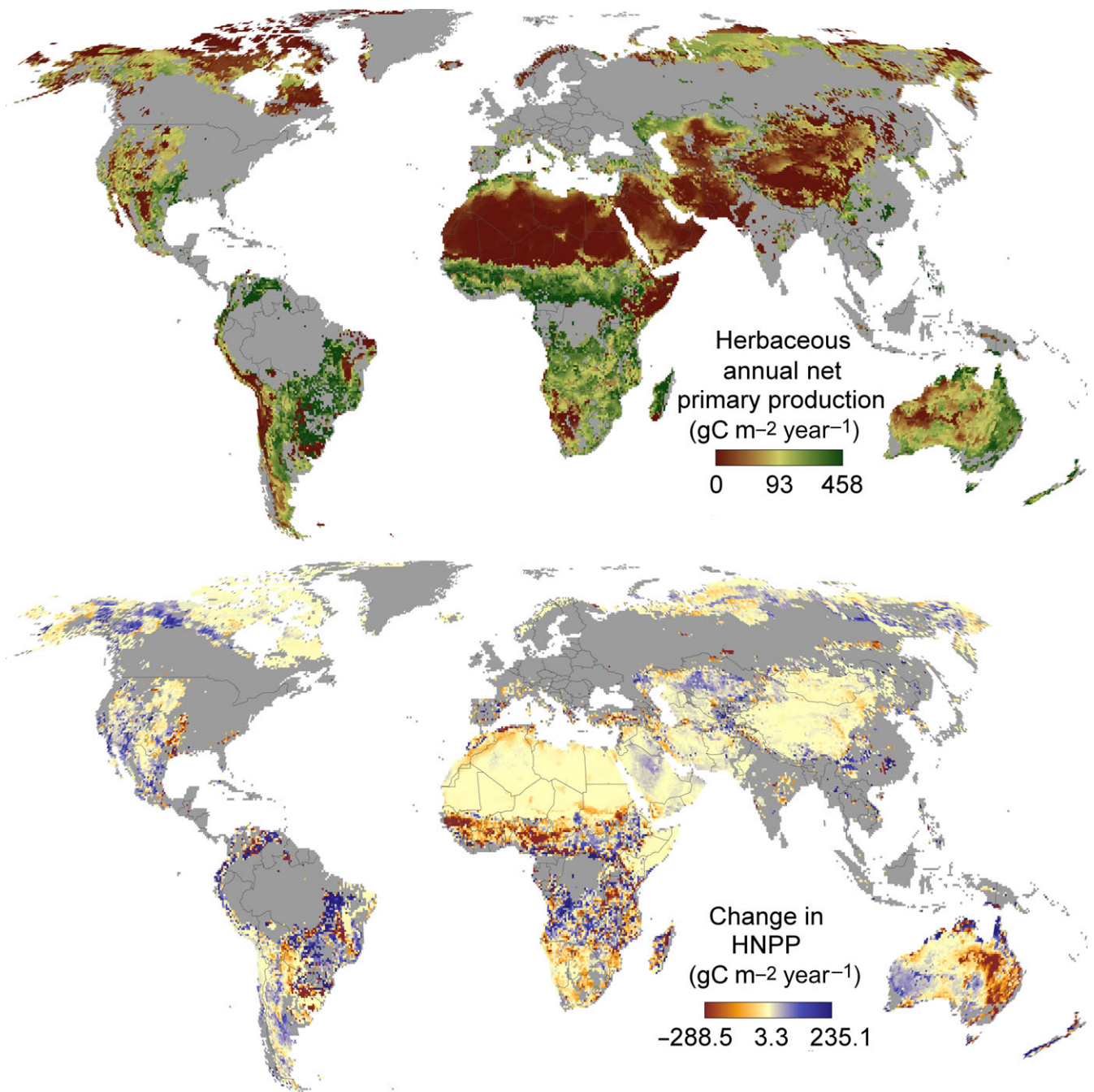


**FIGURE 2** Ensemble simulation results for herbaceous annual net primary productivity of rangelands as simulated in 2000 (top) and their change in 2050 (bottom) under emissions scenario RCP 8.5, with plant responses enhanced by CO<sub>2</sub> fertilization. Scale bar labels and the stretch applied to colors are based on the spatial mean value plus or minus two standard deviations

associated to be due to CO<sub>2</sub> fertilization (Melillo, McGuire, & Kicklighter, 1993). In southern Africa and Australia, bare ground increases following whole plant death at the expense of herbs, shrubs, and trees. In contrast, in northern and western Africa, productivity declines with little mortality or increase in bare ground. In regions with increasing productivity, bare ground often increases modestly; productivity increases in established plant populations rather than through plant population expansion (Figure 3); distinguishing these contradictory changes is a novel aspect of our

modeling approach. Of note is a 44 percent decline in herbaceous cover simulated in East Asia under RCP 8.5, although total productivity is still projected to increase 14 percent.

Total soil organic carbon (SOC) is projected to increase in Australia (9%), the Middle East (14%), and central Asia (16%) and decline in many African savannas (e.g., -18% in sub-Saharan western Africa). Globally, rangeland soil organic carbon to a depth of 60 cm is projected to increase 1.1%. Projected changes in SOC do not always mirror changes in vegetation productivity. Northern

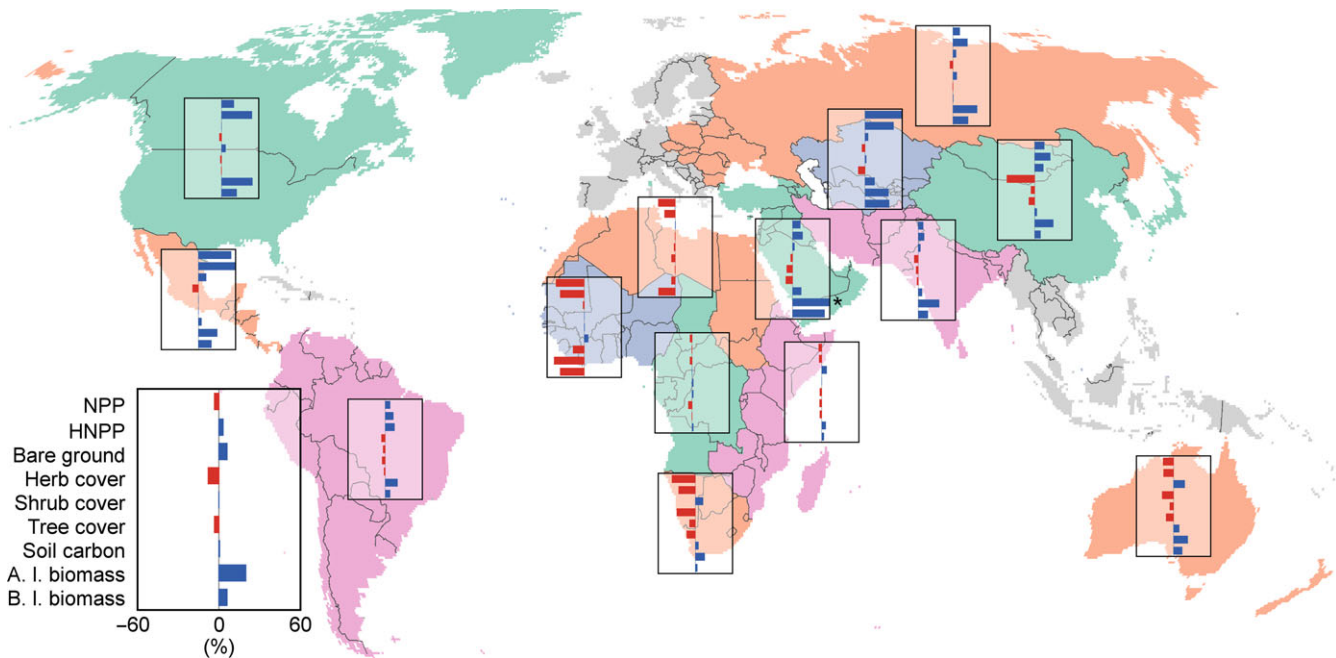


**FIGURE 3** Regional percent changes in selected attributes from ensemble simulation results in 2050 under emissions scenario RCP 85, with plant responses enhanced by CO<sub>2</sub> fertilization. The larger chart (lower left) shows mean changes for all rangelands, and all charts are scaled to −60 to +60 percent change. Shown are annual net primary productivity (NPP), herbaceous net primary productivity (HNPP), bare ground, herbaceous (herb), shrub, and tree cover, soil organic carbon (soil carbon), aboveground live biomass (A. L. biomass), and belowground live biomass (B. L. biomass). Regions were defined by the United Nations Statistics Division. The bar for aboveground live biomass in Western Asia (\*) is truncated and was 82%

temperate rangelands show SOC increases to 60 cm soil depth of 500–1,000 g C/m<sup>2</sup>, similar to simulated estimates for European grasslands (Chang et al., 2015), and parts of Saudi Arabia, the Andes, central Asia, and the Great Plains increased by  $\geq 1000$  g C/m<sup>2</sup>. Declines in SOC of  $\geq 1000$  g C/m<sup>2</sup> were most prevalent in the mesic and semi-arid savannas south of the Sahara, along with eastern Alaska and the Yukon, areas with a decline in NPP and live biomass (Figure 4). In Africa, we project a total decline in soil carbon of 1.36 Gt in 2050, and in the Americas, a decline of 0.35 Gt. In contrast, an increase in total soil carbon in Asia of 1.7 Gt is projected. Globally, in the upper 60 cm of soil in rangelands, we simulated changes in soil organic carbon under RCP 8.5 was projected to increase 1.23 Gt from a baseline of 105.52 Gt.

Globally, bare ground cover is projected to increase, averaging 2.4 percent across rangelands or 7.89E+11 km<sup>2</sup>, with increases projected for the eastern Great Plains, eastern Australia, parts of southern Africa, and the southern Tibetan Plateau (Figure S4a). Herbaceous cover declines in the Tibetan Plateau, the eastern Great Plains, and scattered parts of the Southern Hemisphere (Figure 3). We project declines in shrub cover in eastern Australia, parts of southern Africa, the Middle East, the Tibetan Plateau, and the eastern Great Plains. Shrub cover is projected to increase in much of the Arctic (Pearson et al., 2013) and some parts of Africa. In mesic and semi-arid savannas south of the Sahara, both shrub and tree cover increase, albeit at lower productivity and standing biomass.

Soil degradation and expanding woody cover suggest that climate–vegetation–soil feedbacks catalyzing shifts toward less productive, possibly hysteretically stable states (Ravi, Breshears, Huxman, & D'Odorico, 2010) may threaten mesic and semi-arid savannas south of the Sahara. Woody invasion was accompanied by strong SOC declines in parts of West and southern Africa. Here, reduced herbaceous NPP was associated with SOC losses, suggesting that reduced belowground C allocation from herbs contributed to SOC declines. Mesic and semi-arid (Guinean and Sudanian) savannas south of the Sahara thus appear more prone to SOC loss and soil degradation under woody encroachment than more arid (Sahelian) areas (Barger et al., 2011).

Increased CO<sub>2</sub> concentration is a larger driver of changes in ecosystem carbon stocks than changes in temperature. Simulated ecosystem carbon stocks declined under both climate scenarios without CO<sub>2</sub> effects on productivity, with losses of SOC and belowground biomass exceeding small increases in aboveground biomass (Table 1, Figure 4). In contrast, under elevated CO<sub>2</sub> and corresponding increases in productivity, all three pools increased, with the largest increases in belowground biomass. Storage potential was highest in the southwest United States, the Andes, southern Kazakhstan, and parts of Australia, and weakest in Africa. In some areas of southern and East Africa, herbaceous and woody plants contribute to carbon storage potential, while gains in the Sahara and Middle East come primarily from herbaceous vegetation.



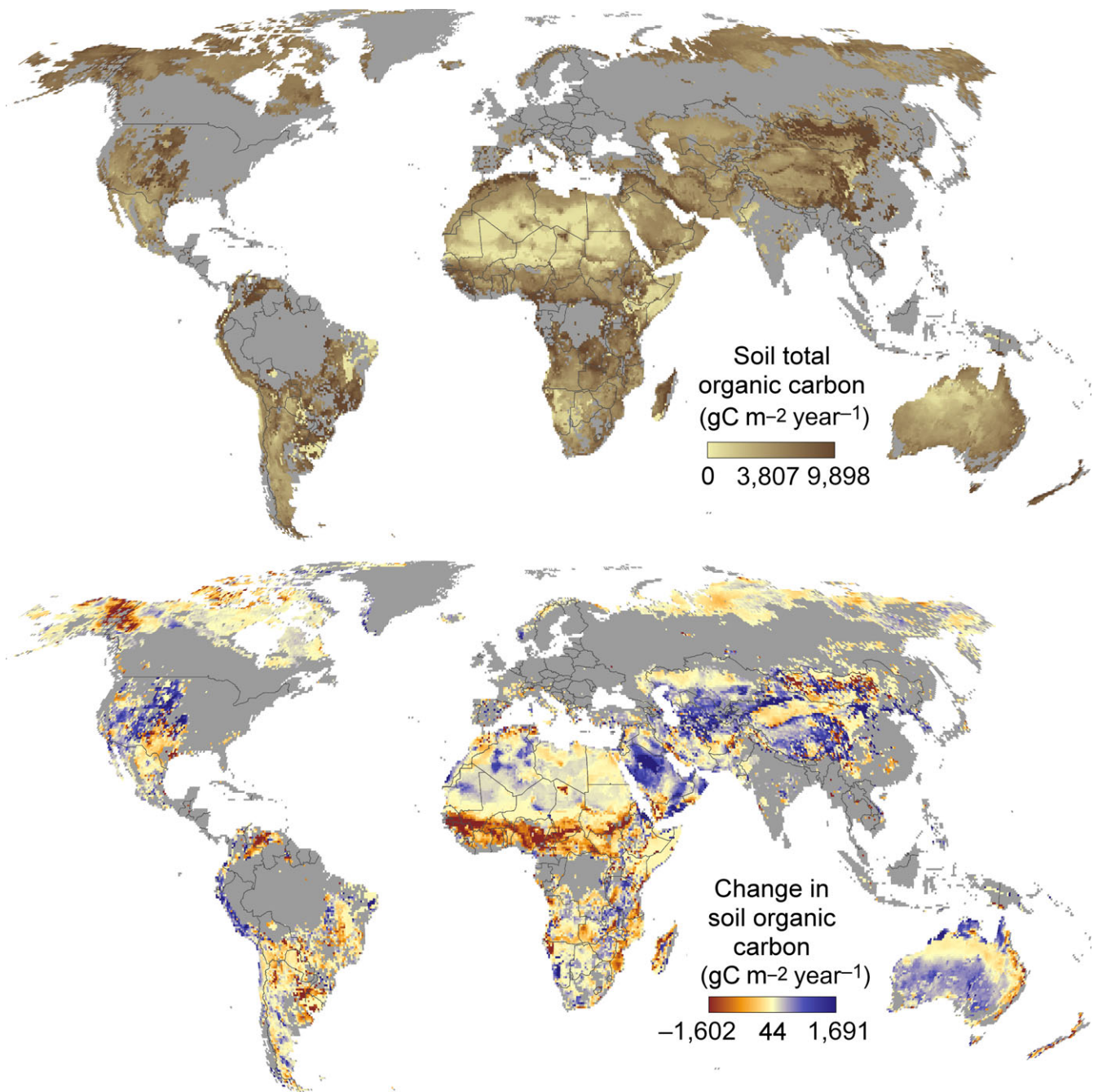


**FIGURE 4** Ensemble simulation results for soil organic carbon to 60 cm depth in rangelands as simulated in 2000 and their change in 2050 under emissions scenario RCP 8.5, with plant responses enhanced by CO<sub>2</sub> fertilization. Scale bar labels and the stretch applied to colors are based on the spatial mean value plus or minus two standard deviations

Our results show that ecosystem services we quantified from rangelands (e.g., NPP, HNPP, carbon storage) will decline to the middle of the century in much of Africa, eastern Australia, and parts of the Americas. Globally, based on changes in herbaceous production under RCP 8.5, grazing livestock are projected to decline by 28.7 to 37.1 million livestock units (i.e., 250 kg body mass) or 7.5 to 9.6% of total stocking in rangelands, representing an economic loss of between \$9.7 and \$12.6 billion. Declines are most palpable in savannas south of the Sahara, where declining forage and browse

production present significant climate-induced threats to rangeland production systems. Currently, re-greening areas of western Africa (Dardel et al., 2014) are among those we find to be vulnerable to climate-induced degradation (i.e., after re-greening ceases), as are areas that are currently degrading. Some areas degraded by management in southern (Dubovyk, Landmann, Erasmus, Tewes, & Schellberg, 2015; Prince, Becker-Reshef, & Rishmawi, 2009) and East Africa (Dubovyk et al., 2015) overlap those we project as being vulnerable to climate change, portending interaction among degradation risks.



## 4 | DISCUSSION

Given the close relationships linking NPP and HNPP with livestock production, productivity and profitability (Moore & Ghahramani, 2013), these results are particularly worrying for Africa. Despite their uncertainty, they imply that substantial changes in livestock feed resources will occur in this century, and in large parts of the continent, these changes will be detrimental. At the same time, demand for livestock products is increasing, as in many parts of the world, and is projected to nearly double in sub-Saharan Africa by 2050 (Alexandratos & Bruinsma, 2012). Various adaptation avenues exist for livestock keepers in African rangelands and elsewhere, such as genetic selection for more heat- and drought-tolerant animals, adaptive management of resources and diversity at the farm level, improved animal health measures, conversion of some rangelands to cropping, and income or livestock insurance schemes, and market development (Thornton, 2010). All such options have significant constraints to their wide adoption, however, and their feasibility will depend on local conditions and the costs of their implementation, among other things (Thornton & Herrero, 2014). Some livestock adaptation changes may involve transformation of farmers' livelihoods, such as the adoption of camels and goats as a replacement for cattle in drylands as a result of changing drought frequency and the changes projected here in the balance between herbs and shrubs, altering the suitability of the rangelands for different types of animals (e.g., browsers versus grazers). Other options for increasing incomes include market-based payment schemes, aimed at compensating pastoralists for the production of rangeland environmental services that benefit others (Reid, Fernandez-Gimenez, & Galvin, 2014). While schemes exist for wildlife, water and carbon, for example, widespread implementation has many challenges.

Caveats in interpreting our results include that uncertainties in simulating monthly climate into the future are inherent here and that productivity of rangelands in a changing climate depends upon sometimes small differences in temperature, precipitation, its variability, CO<sub>2</sub> concentration, and nutrient availability, making outcomes uncertain. In general, biochemical and plant production modeling is informed by the long history of the CENTURY model (Parton et al., 1993; Figure S2 reports fit). In contrast, population dynamics modeling includes estimates of seed production and effects on establishment and whole plant death rate. Attributes limiting plant establishment or whole plant death in a 2050 climate are not known. The streamlined nature of G-Range limits the detail that may be represented in the model. However, users may define homogeneous landscape units for which parameters are provided in as detailed a manner as they wish. For example, our parameterization reflects different compositions of C<sub>3</sub> and C<sub>4</sub> plants in the biomes used. Fire extent and frequencies are stochastic in the current application and based on observed frequencies, but may be expected to increase (Running, 2006).

The effects of climate change on rangelands, their ecosystem services and functions, and human well-being are complex. We have little information on the possible costs and benefits (both social and

private) of changes in these systems or their likely impacts on human development outcomes. An approach such as that presented here, especially if it can incorporate human well-being and livestock energy and population dynamics, offers considerable potential for generating some of the information needed. Otherwise, the technical options and policy and enabling environment that are needed to facilitate widespread adaptation may be very difficult to elucidate.

We project NPP to increase in North America and Central America, and Central Asia. Large decreases are projected for much of Africa and portions of Australia. Soil carbon is projected to decrease in Africa, and we may see a more modest increase in Asia. Declines in herbaceous plants and increases in bare ground are forecast for temperate grasslands in North America and Asia. An overarching result is the large spatial variability seen in the ecosystem service surfaces created. As our atmosphere warms and precipitation becomes more variable, rangeland inhabitants will include both winners and losers. The spatial distribution of livestock production and corresponding markets may be expected to shift and populations already food insecure may become increasingly so.

## ACKNOWLEDGEMENTS

We thank Peter G. Jones for climate data input and those who have contributed to the global circulation model results we used in the analyses. Funding has been provided by the International Livestock Research Institute, Nairobi, Kenya and the CGIAR Research Program on Climate Change, Agriculture and Food Security (CCAFS). CCAFS is funded by the CGIAR Fund Council, European Union, the International Fund for Agricultural Development. Publishing support was provided by the National Science Foundation under grant BCS-1733817. P.K.T. acknowledges the support of a CSIRO McMaster Research Fellowship.

## CONFLICT OF INTEREST

The authors declare no conflict of interest.

## AUTHOR CONTRIBUTIONS

R.B.B. created G-Range and conducted analyses; R.T.C. and J.S. contributed to project development and J.S. and M.H. conducted analyses; P.K.T., R.T.C., and M.H. conceived analyses and P.K.T. provided climate data; R.B.B. prepared the initial manuscript and all authors contributed to revisions.

## ORCID

Randall B. Boone  <http://orcid.org/0000-0003-3362-2976>

## REFERENCES

- Alexandratos, N., & Bruinsma, J. (2012). *World agriculture towards 2030/2050: The 2012 revision*. Rome, Italy. ESA Working Paper No. 12-03. Food and Agriculture Organization of the United Nations.

- Armstrong, R., Brodzik, M. J., Knowles, K., & Savoie, M. (2005). *Global monthly EASE-Grid snow water equivalent climatology: Snow water equivalent*. Boulder, CO: National Snow & Ice Data Center.
- Barger, N. N., Archer, S. R., Campbell, J. L., Huang, C., Morton, J. A., & Knapp, A. K. (2011). Woody plant proliferation in North American drylands: A synthesis of impacts on ecosystem carbon balance. *Journal of Geophysical Research*, 116, G00K07.
- Batjes, N. H. (2002). Revised soil parameter estimates for the soil types of the world. *Soil Use and Management*, 18, 232–235. <https://doi.org/10.1111/j.1475-2743.2002.tb00244.x>
- Birdsey, R., Mickler, R., Sandberg, D., Tinus, R., Zerbe, J., & O'Brian, K. (Eds.) (1997). *USDA forest service global change research program highlights: 1991–1995: Effects of global change*. General Technical Report NE-237. Radnor, PA: US Department of Agriculture Forest Service, Northeastern Forest Experiment Station.
- Boone, R. B., BurnSilver, S. B., Thornton, P. K., Worden, J. S., & Galvin, K. A. (2005). Quantifying declines in livestock due to subdivision. *Rangeland Ecology & Management*, 58, 523–532. [https://doi.org/10.2111/1551-5028\(2005\)58\[523:QDILDT\]2.0.CO;2](https://doi.org/10.2111/1551-5028(2005)58[523:QDILDT]2.0.CO;2)
- Boone, R. B., Conant, R. T., & Hilinski, T. E. (2011). *G-Range: Development and use of a beta global rangeland model* (p. 66). Fort Collins, CO: Colorado State University.
- Boone, R. B., Conant, R. T., & Sircely, J. (2013). *Adjustment and sensitivity analyses of a beta global rangeland model* (p. 140). Fort Collins, CO: Colorado State University.
- Boone, R. B., Coughenour, M. B., Galvin, K. A., & Ellis, J. E. (2002). Addressing management questions for Ngorongoro conservation area using the savanna modeling system. *African Journal of Ecology*, 40, 138–150. <https://doi.org/10.1046/j.1365-2028.2002.00357.x>
- Boone, R. B., Galvin, K. A., BurnSilver, S. B., Thornton, P., Ojima, D., & Jawson, J. (2011). Using coupled simulation models to link pastoral decision making and ecosystem services. *Ecology and Society*, 16(2), 6. <http://www.ecologyandsociety.org/vol16/iss2/art6/>
- Boone, R. B., & Lesoroog, C. K. (2016). Modelling coupled human-natural systems of pastoralism in East Africa. In S. Dong, K.-A. S. Kassam, J. F. Tourrand, & R. B. Boone (Eds.), *Pastoralism in the developing world: An exploration of interdisciplinary strategies for sustainable pastoralism* (pp. 251–280). Cham, Switzerland: Springer.
- Chang, J., Ciaia, P., Viovy, N., Vuichard, N., Sultan, B., & Soussana, J.-F. (2015). The greenhouse gas balance of European grasslands. *Global Change Biology*, 21, 3748–3761. <https://doi.org/10.1111/gcb.12998>
- Collier, M. A., Jeffrey, S. J., Rotstayn, L. D., Wong, K. K., Dravitzki, S. M., Moseneder, C., & El Zein, A. (2011). The CSIRO-Mk3.6.0 atmosphere-ocean GCM: participation in CMIP5 and data publication. In F. Chan, D. Marinova, & R. S. Anderssen (Eds.), *19th international congress on modelling and simulation* (pp. 2691–2697). Perth, WA: Modelling and Simulation Society of Australia and New Zealand.
- Collins, W. J., Bellouin, N., Doutriaux-Boucher, M., Gedney, N., Halloran, P., Hinton, T., ... Woodward, S. (2011). Development and evaluation of an Earth-System model – HadGEM2. *Geoscientific Model Development*, 4, 1051–1075. <https://doi.org/10.5194/gmd-4-1051-2011>
- Coughenour, M. B. (1992). Spatial modeling and landscape characterization of an African pastoral ecosystem: A prototype model and its potential use for monitoring drought. In D. H. McKenzie, D. E. Hyatt, & V. J. McDonald (Eds.), *Ecological indicators* (pp. 787–810). New York, NY: Springer. <https://doi.org/10.1007/978-1-4615-4659-7>
- Dardel, C., Kergoat, L., Hiernaux, P., Mougou, E., Grippa, M., & Tucker, C. J. (2014). Re-greening Sahel: 30 years of remote sensing data and field observations (Mali, Niger). *Remote Sensing of Environment*, 140, 350–364. <https://doi.org/10.1016/j.rse.2013.09.011>
- de Leeuw, J., Osano, P., Said, M. Y., Ayantunde, A. A., Dube, S., Neely, C., ... Thornton, P. K. (in press). Pastoral farming systems and food security in Sub-Saharan Africa Priorities for science and policy. In J. Dixon et al. (Eds.), *Farming Systems and Food Security in Africa: Priorities for science and policy under global change*. London, UK: Routledge.
- DeFries, R. S., Hansen, M. C., Townshend, R. G., Janetos, A. C., & Loveland, T. R. (2000). A new global 1-km dataset of percentage tree cover derived from remote sensing. *Global Change Biology*, 6, 247–254. <https://doi.org/10.1046/j.1365-2486.2000.00296.x>
- Derry, J. F. (2005). *Piospheres in semi-arid rangeland: Consequences of spatially constrained plant-herbivore interactions*. Ph.D. thesis, Edinburgh, UK: University of Edinburgh.
- Donner, L. J., Wyman, B. L., Hemler, R. S., Horowitz, L. W., Ming, Y., Zhao, M., ... Zeng, F. (2011). The dynamical core, physical parameterizations, and basic simulation characteristics of the atmospheric component AM3 of the GFDL Global Coupled Model CM3. *Journal of Climate*, 24, 3484–3519. <https://doi.org/10.1175/2011JCLI3955.1>
- Dubovyk, O., Landmann, T., Erasmus, B. F. N., Tewes, A., & Schellberg, J. (2015). Monitoring vegetation dynamics with medium resolution MODIS-EVI time series at sub-regional scale in southern Africa. *International Journal of Applied Earth Observation and Geoinformation*, 38, 175–183. <https://doi.org/10.1016/j.jag.2015.01.002>
- Dufresne, J.-L., Foujols, M.-A., Denvil, S., Caubel, A., Marti, O., Aumont, O., ... Vulchard, N. (2013). Climate change projections using the IPSL-CM5 Earth System Model: From CMIP3 to CMIP5. *Climate Dynamics*, 40, 2123–2165. <https://doi.org/10.1007/s00382-012-1636-1>
- Erb, K.-H., Lauk, C., Kastner, T., Mayer, A., Theuri, M., & Haberl, H. (2016). Exploring the biophysical option space for feeding the world without deforestation. *Nature Communication*, 7, 11382. <https://doi.org/10.1038/ncomms11382>
- FAO (FAO, IASA, ISRIC, ISS-CAS, JRC) (2012). *Harmonized world soil database*. Rome, Italy: Food and Agricultural Organization of the United Nations.
- Foley, J. A., Prentice, I. C., Ramankutty, N., Levis, S., Pollard, D., Sitch, S., & Haxeltine, A. (1996). An integrated biosphere model of land surface processes, terrestrial carbon balance, and vegetation dynamics. *Global Biogeochemical Cycles*, 10, 603–628. <https://doi.org/10.1029/96GB02692>
- Giglio, L., Randerson, J. T., van der Werf, G. R., Kasibhatla, P. S., Collatz, G. J., Morton, D. C., & DeFries, R. S. (2010). Assessing variability and long-term trends in burned area by merging multiple satellite fire products. *Biogeosciences*, 7, 1171–1186. <https://doi.org/10.5194/bg-7-1171-2010>
- Hansen, M., DeFries, R., Townshend, J. R., Carroll, M., Dimiceli, C., & Sohlberg, R. (2006). *Vegetation Continuous Fields MOD44B, 2001 percent tree cover*. College Park, MD: University of Maryland.
- Henderson, B. B., Gerber, P. J., Hilinski, T. E., Falcucci, A., Ojima, D. S., Salvatore, M., & Conant, R. T. (2015). Greenhouse gas mitigation potential of the world's grazing lands: Modeling soil carbon and nitrogen fluxes of mitigation practices. *Agriculture, Ecosystems & Environment*, 207, 91–100. <https://doi.org/10.1016/j.agee.2015.03.029>
- Herrero, M., Havlík, P., Valin, H., Notenbaert, A., Rufino, M. C., Thornton, P. K., ... Obersteiner, M. (2013). Biomass use, production, feed efficiencies, and greenhouse gas emissions from global livestock systems. *Proceedings of the National Academy of Sciences of the United States of America*, 110, 20888–20893. <https://doi.org/10.1073/pnas.1308149110>
- Herrero, M., Wiersma, S., Henderson, B., Rigolot, C., Thornton, P., Havlík, P., & de Boer, I. (2013). Livestock and the environment: What have we learned in the last decade? *Annual Review of Environment and Resources*, 40, 177–202.
- Hobbs, N. T., Galvin, K. A., Stokes, C. J., Lockett, J. M., Ash, A. J., Boone, R. B., ... Thornton, P. K. (2008). Fragmentation of rangelands: Implications for humans, animals, and landscapes. *Global Environmental Change*, 18, 776–785. <https://doi.org/10.1016/j.gloenvcha.2008.07.011>
- IPCC (Intergovernmental Panel on Climate Change) (2014). *Climate Change 2014: Synthesis Report. Contribution of Working Groups I, II and III to the fifth Assessment Report of the Intergovernmental*

- Panel on Climate Change [Core Writing Team, R.K. Pachauri and L.A. Meyer (Eds.)]. Geneva, Switzerland, 151 pp.
- King, D. A., Bachelet, D. M., & Symstad, A. J. (2013). Climate change and fire effects on a prairie-woodland ecotone: Projecting species range shifts with a dynamic global vegetation model. *Ecology and Evolution*, 3, 5076–5097. <https://doi.org/10.1002/ece3.877>
- Loveland, T. R., Reed, B. C., Brown, J. F., Ohlen, D. O., Zhu, J., Yang, L., & Merchant, J. W. (2000). Development of a global land cover characteristics database and IGBP DISCover from 1-km AVHRR data. *International Journal of Remote Sensing*, 21, 1303–1330. <https://doi.org/10.1080/014311600210191>
- Meinshausen, M., Smith, S. J., Calvin, K., Daniel, J. S., Kainuma, M. L. T., Lamarque, J. F., ... van Vuuren, D. P. P. (2011). The RCP greenhouse gas concentrations and their extensions from 1765 to 2300. *Climatic Change*, 109, 213–241. <https://doi.org/10.1007/s10584-011-0156-z>
- Melillo, J., McGuire, A., & Kicklighter, D. (1993). Global climate change and terrestrial net primary production. *Nature*, 363, 234–240. <https://doi.org/10.1038/363234a0>
- Mitchell, T. D., & Jones, P. D. (2005). An improved method of constructing a database of monthly climate observations and associated high-resolution grids. *International Journal of Climatology*, 25, 693–712. [https://doi.org/10.1002/\(ISSN\)1097-0088](https://doi.org/10.1002/(ISSN)1097-0088)
- Moore, A. D., & Ghahramani, A. (2013). Climate change and broadacre livestock production across southern Australia. 1. Impacts of climate change on pasture and livestock productivity, and on sustainable levels of profitability. *Global Change Biology*, 19, 1440–1455. <https://doi.org/10.1111/gcb.12150>
- Moorhead, D., & Reynolds, J. (1991). A general model of litter decomposition in the northern Chihuahua Desert. *Ecological Modelling*, 56, 197–219. [https://doi.org/10.1016/0304-3800\(91\)90200-K](https://doi.org/10.1016/0304-3800(91)90200-K)
- Moss, R., Babiker, M., Brinkman, S., Calvo, E., Carter, T., Edmonds, J., ... Zurek, M. (2008). *Towards new scenarios for analysis of emissions, climate change, impacts, and response strategies*. Technical Summary. (p. 132). Geneva, Switzerland: Intergovernmental Panel on Climate Change.
- Pan, Y., Melillo, J., McGuire, A. D., Kicklighter, D. W., Pitelka, L. F., Hibbard, K., Schimel, D. S. (1998). Modeled responses of terrestrial ecosystems to elevated atmospheric CO<sub>2</sub>: A comparison of simulations by the biogeochemistry models of the Vegetation/Ecosystem Modeling and Analysis Project (VEMAP) on JSTOR. *Oecologia*, 114, 389–404. <https://doi.org/10.1007/s004420050462>
- Parton, B., Ojima, D., Del Grosso, S., & Keough, C. (2001). *CENTURY tutorial: Supplement to CENTURY user's manual* (p. 140). Fort Collins, CO: Colorado State University.
- Parton, W. J., Scurlock, J. M. O., Ojima, D. S., Gilmanov, T. G., Scholes, R. J., Schimel, D. S., ... Kinyamario, J. L. (1993). Observations and modeling of biomass and soil organic matter dynamics for the grassland biome worldwide. *Global Biogeochemical Cycles*, 7, 785–809. <https://doi.org/10.1029/93GB02042>
- Pearson, R. G., Phillips, S. J., Loran, M. M., Beck, P. S. A., Damoulas, T., Knight, S. J., Goetz, S. J. (2013). Shifts in Arctic vegetation and associated feedbacks under climate change. *Nature Climate Change*, 3, 673–677. <https://doi.org/10.1038/nclimate1858>
- Prince, S. D., Becker-Reshef, I., & Rishmawi, K. (2009). Detection and mapping of long-term land degradation using local net production scaling: Application to Zimbabwe. *Remote Sensing of Environment*, 113, 1046–1057. <https://doi.org/10.1016/j.rse.2009.01.016>
- Ramankutty, N., & Foley, J. A. (1999). Estimating historical changes in global land cover: Croplands from 1700 to 1992. *Global Biogeochemical Cycles*, 13, 997–1027. <https://doi.org/10.1029/1999GB900046>
- Ravi, S., Breshears, D. D., Huxman, T. E., & D'Odorico, P. (2010). Land degradation in drylands: Interactions among hydrologic–aeolian erosion and vegetation dynamics. *Geomorphology*, 116, 236–245. <https://doi.org/10.1016/j.geomorph.2009.11.023>
- Reid, R. S., Fernandez-Gimenez, M. E., & Galvin, K. A. (2014). Dynamics and resilience of rangelands and pastoral peoples around the globe. *Annual Review of Environment and Resources*, 39, 217–242. <https://doi.org/10.1146/annurev-environ-020713-163329>
- Reid, R. S., Galvin, K. A., & Kruska, R. S. (2008). Global significance of extensive grazing lands and pastoral societies: An introduction. In K. A. Galvin, R. S. Reid, R. H. Behnke, & N. T. Hobbs (Eds.), *Fragmentation in semi-arid and arid landscapes: Consequences for human and natural systems* (pp. 1–24). Dordrecht, The Netherlands: Springer. <https://doi.org/10.1007/978-1-4020-4906-4>
- Robinson, T., Thornton, P., Franceschini, G., Kruska, R. L., Chiozza, F., Notenbaert, A. M. O., ... See, L. (2011). *Global livestock production systems*. Rome, Italy: Food and Agricultural Organization of the United Nations and International Livestock Research Institute.
- Robinson, T. P., Wint, G. R. W., Conchedda, G., Van Boeckel, T. P., Ercoli, V., Palamara, E., ... Gilbert, M. (2014). Mapping the global distribution of livestock. *PLoS One*, 9, e96084. <https://doi.org/10.1371/journal.pone.0096084>
- Rosegrant, M. W., Fernandez, M., Sinha, A., Alder, J., Ahammad, H., Fraiture, C. D., ... Yana-Shapiro, H. (2009). Looking into the future for agriculture and AKST. In B. D. McIntyre, H. R. Herren, J. Wakhungu, & R. T. Watson (Eds.), *International assessment of agricultural knowledge, science and technology for development (IAASTD): Agriculture at a crossroads, global report* (pp. 307–376). Washington, DC: Island Press.
- Ruesch, A., & Gibbs, H. K. (2008). *New IPCC Tier-1 global biomass carbon map for the year 2000*. Oak Ridge, TN: Oak Ridge National Laboratory.
- Running, S. W. (2006). Climate change. Is global warming causing more, larger wildfires? *Science*, 313, 927–928. <https://doi.org/10.1126/science.1130370>
- Schmidt, G. A., Ruedy, R., Hansen, J. E., Aleinov, I., Bell, N., Bauer, M., ... Yao, M.-S. (2006). Present-day atmospheric simulations using GISS ModelE: Comparison to *in situ*, satellite, and reanalysis data. *Journal of Climate*, 19, 153–192. <https://doi.org/10.1175/JCLI3612.1>
- Sietse, O. L. (2010). ISLSCP II FASIR-adjusted NDVI Biophysical Parameter Fields, 1982–1998. In F. G. Hall, G. Collatz, B. Meeson, S. Los, E. Brown de Colstoun, & D. Landis (Eds.), *ISLSCP Initiative II Collection*. Data set. Oak Ridge, TN: Oak Ridge National Laboratory Distributed Active Archive Center. Hall. Available online [http://daac.ornl.gov/].
- Stuth, J. W., Connor, J. R., Hamilton, W. T., Riegel, D. A., Lyons, B. G., Myrick, B. R., & Couch, M. J. (1990). RSPM: A resource systems planning model for integrated resource management. *Journal of Biogeography*, 17, 531–540. <https://doi.org/10.2307/2845387>
- Stuth, J. W., Schmitt, D., Rowan, R., Angerer, J. P., & Zander, K. (2003). *PHYGROW users guide and technical documentation*. College Station, TX: Texas A&M University.
- Thornley, J. (1997). Temperate grassland responses to climate change: An analysis using the Hurley pasture model. *Annals of Botany*, 80, 205–221. <https://doi.org/10.1006/anbo.1997.0430>
- Thornton, P. K. (2010). Livestock production: Recent trends, future prospects. *Philosophical transactions of the Royal Society of London. Series B, Biological Sciences*, 365, 2853–2867. <https://doi.org/10.1098/rstb.2010.0134>
- Thornton, P. K., & Herrero, M. (2014). Climate change adaptation in mixed crop–livestock systems in developing countries. *Global Food Security*, 3, 99–107. <https://doi.org/10.1016/j.gfs.2014.02.002>
- Thornton, P. E., Law, B. E., Gholz, H. L., Clark, K. L., Falge, E., Ellsworth, D. S., ... Sparks, J. P. (2002). Modeling and measuring the effects of disturbance history and climate on carbon and water budgets in evergreen needleleaf forests. *Agriculture and Forest Meteorology*, 113, 185–222. [https://doi.org/10.1016/S0168-1923\(02\)00108-9](https://doi.org/10.1016/S0168-1923(02)00108-9)
- Wu, T. (2012). A mass-flux cumulus parameterization scheme for large-scale models: Description and test with observations. *Climate Dynamics*, 38, 725–744. <https://doi.org/10.1007/s00382-011-0995-3>



- Yukimoto, S., Adachi, Y., Hosaka, M., Sakami, T., Yoshimura, H., Hirabara, M., ... Kitoh, A. (2012). A new global climate model of the Meteorological Research Institute: MRI-CGCM3; model description and basic performance. *Journal of the Meteorological Society of Japan*, 90A, 23–64. <https://doi.org/10.2151/jmsj.2012-A02>
- Zhang, K., Kimball, J. S., Nemani, R. R., & Running, S. W. (2010). A continuous satellite-derived global record of land surface evapotranspiration from 1983 to 2006. *Water Resources Research*, 46, W09522.
- Zhao, M., Running, S., Heinsch, F. A., & Nemani, R. (2011). MODIS-derived terrestrial primary production. In B. Ramachandran, C. O. Justice, & M. J. Abrams (Eds.), *Land remote sensing and global environmental change*, vol. 11 (pp. 635–660). New York, NY: Springer.

## SUPPORTING INFORMATION

Additional Supporting Information may be found online in the supporting information tab for this article.

**How to cite this article:** Boone RB, Conant RT, Sircely J, Thornton PK, Herrero M. Climate change impacts on selected global rangeland ecosystem services. *Glob Change Biol.* 2017;00:1–12. <https://doi.org/10.1111/gcb.13995>